Numerical modelling of long waves in wide rectangular channels in lagrangian coordinates

Anatoly Krutov

N.N.'s Zubov State Oceanographic Institute, Roshydromet, Moscow, Russia

Abstract. The paper discusses the possibility of using Lagrangian coordinates to predict the transformation of long waves of different origins near the coasts, necessary in the design, construction, and operation of protective structures, as well as a wide range of environmental problems related, among others, to the spread of pollutants. Results of numerical investigations, compared with analytical solutions, showed satisfactory coincidence.

1 Introduction

*Engineering problems a*ssociated with the propagation of long waves and their interaction with hydraulic structures require hydrodynamic calculations of currents in areas with variable boundaries where it is necessary to predict:

- transformation of surge, tidal, and tsunami waves coastal security;
- breakwater and flood propagation parameters
- water movement during furrow irrigation;

or carry out

- ecological assessments of shallow waters and coastal marshes
- predicting HPP-PSPP operation regimes.

The most common mathematical model for solving hydrodynamic problems in shallow unstratified open water bodies is the Saint-Venant equation (Stoker J.J., 1959, Wiseman J., 1997, Wolzinger N.E., Pyaskovsky R.V., J. A. Künge, F. M. Holly, A. Verwey., 1985, D.A. Drew, 1983, J.F. Gerbeau, B. Perthame, 2001, T. Buffard, T. Gallouet, J.M. H´erard, 1998). Two approaches are commonly used to solve problems with variable boundaries:

- pass-through method (Belikov V.V., Norin S.V., Shkolnikov S.Ya., 2014)
- methods related to separating boundaries and developing movable grids (V.M. Lyatkher, Y.S. Yakovlev, 1976).

Three approaches for implementing pass-through methods are described in (Fedotova Z.I., 2002):

- on land, a thin film of water held on the surface by frictional force is assumed,
- a body of water of simple geometry is embedded into the area occupied by land,

- In the non-flooded area, the depth and flow velocity are set to zero.

In pass-through, the calculations are carried out in Eulerian coordinates.
In the case of boundary selection, coordinates that are not purely Euler coordinates but some coordinate's line that moves with the boundary of the computational domain(Belikov V.V., Norin S.V., Shkolnikov S.Ya., 2014).
The motivation for this research was to overcome the problem of separating the physical and schematic diffusion of a fluid using Eulerian coordinates in numerical calculations of wave processes and also the fact of wide application of computational methods using Lagrangian coordinates in the solution of gas dynamics problems in regions with variable boundaries (Samarskiy A.A., Popov Yu.P., 1992).

The following is an explicit finite-difference method for calculating wave currents off the coast, using Lagrangian coordinates under the assumption of planar symmetry.

2 Methods and Materials

2.1 Saint-Venin equations in Lagrangian coordinates

Currently, the most widely used mathematical model describing currents in open unstratified bodies of water is the Saint-Venin system of equations. This system is based on the hypothesis of hydrostatic pressure distribution over depth. As a rule (not always), this hypothesis is supplemented by the hypothesis that the velocity epure is close to a rectangular one and that the friction laws used in steady-state currents apply to unsteady currents.

The Saint-Venin equations in Lagrange coordinates assuming planar symmetry can be represented in integral form (Krutov, A.N. Shkolnikov, S.Ya., 2022):

$$\begin{cases} \int\limits_{X_0}^{X_1} h dx \Big|_{t_0}^{t_1} = 0, \quad X_{0;1} = X\left(t, \hat{X}_{0;1}\right), \\ \int\limits_{X_0}^{X_1} q dx \Big|_{t_0}^{t_1} = \int\limits_{t_0}^{t_1} \frac{gh^2}{2} dt \Big|_{\tilde{X}_0}^{\tilde{X}_1} + \int\limits_{t_0}^{t_1} dt \int\limits_{X_0}^{X_1} \left(R + \Theta + \Phi\right) q dx \Big|, \\ q = q\left(t, \hat{X}\right), \quad h = h\left(t, \hat{X}\right), \quad R = R\left(t, \hat{X}\right), \quad \Theta = \Theta\left(t, \hat{X}\right), \end{cases} \tag{1}$$

$X\left(t, \hat{X}\right)$ is the spatial Eulerian coordinate of the station moving with the fluid flow, linked with the Lagrangian coordinate of the station by the relation:

$$X = \hat{X} + \int\limits_0^t V dt, \tag{2}$$

$V\left(t, \hat{X}\right)$ is velocity of liquid particles, q is specific water flow, h is depth, g=9,8 m/s is acceleration of gravity, $\rho \frac{gh^2}{2}$ is hydrostatic pressure divided by width unit, ρ is liquid density, ρR is the projection onto the X axis of the pressure acting from the bottom on the fluid, numerically equal to the projection onto the same axis of the fluid pressure on the bottom of the stream, opposite in direction to it,

$$R = gh\frac{dZ_b}{dX} = -ghI = -g\frac{\partial h^2/2}{\partial x}_{|Z_{fs}=const} \quad (3)$$

Z_b is stream bottom mark, not changing in time in Eulerian coordinates, $I = -\frac{dZ_b}{dX}$ is bottom slope, $\rho\Theta$ is hydraulic friction stress at the bottom of the stream, using the Darcy-Weisbach formula (McKeon, B. J.; Zagarola, M. V; Smits, A. J. 2005:

$$\Theta = \frac{\lambda}{2}V|V| \quad (4)$$

λ is coefficient of hydraulic friction using Manning's formula (Manning, R., 1891, Gauckler, Ph. 1867):

$$\lambda = 2gn^2/h^{1/3} \quad (5)$$

n is bottom roughness coefficient, the value of which depends on the underlying surface (Kiselev P.G. (ed.), 1974), ρ, Φ is other forces affecting the flow: wind stress on the free water surface, projection of the tidal force on the flow axis, etc. In this paper, it is assumed that the influence of these forces is negligible and Φ is not taken into account further in the calculations.

The first equation of the system (1) expresses the law of conservation of mass of an incompressible fluid; the second equation is the law of conservation of momentum for this fluid.

Note that, for flows in areas with variable boundaries, drying of zones within an initially single-bonded area is possible. Such phenomena are not considered in this paper.

2.2 Numerical implementation of the Saint-Venin equations in Lagrangian coordinates without bottom topography and friction

In (Krutov, A.N. Shkolnikov, S.Ya., 2022), an explicit finite-difference scheme for a channel without gradient and friction and without considering the bottom relief is proposed, implementing (1.1), in which the value *R*=0 has the following form:

$$\begin{cases} h_k^1\left(X_{k+1/2}^1 - X_{k-1/2}^1\right) = \Delta_{\Omega k}, \\ X_{k+1/2}^1 = X_{k+1/2} + \tau V_{k+1/2}, \\ V_{k+1/2}^1 = V_{k+1/2} - \dfrac{\tau g}{\Delta_{\Omega k} + \Delta_{\Omega k+1}}\left(h_{k+1}^{1\ 2} - h_k^{1\,2}\right), \end{cases} \quad (6)$$

here: subscript *k*: $1 \le k \le K$ is cell number of the finite-difference scheme, fractional lower index (subscript) *k*+1/2 indicates that the corresponding value is assigned to the boundary between *k*-th and *k*+1-th cells, τ is time step,

$$\Delta_{\Omega k} = h_k\left(X_{k+1/2} - X_{k-1/2}\right) \quad - \quad (7)$$

is specific (by flow width) fluid volume in *k*-th cell of the finite-difference scheme, located

between moving sections and $X_{k-1/2}$ and $X_{k+1/2}$; $\Delta_{\Omega k}$ does not change with time and can be calculated once, at the beginning of calculations; hereinafter the values with upper index "1" refer to a new time step, without indices - to the old one, scheme parameters of flow are marked the same way as their analogs in the description of the mathematical model in section 1.

The proposed explicit finite-difference scheme (6) has a time step limit Courant condition (R. Courant, K. Friedrichs, H. Lewyt ,1928.):

$$\tau < \min_{\forall k:1\le k\le K}\left(2\frac{X_{k+1/2}-X_{k-1/2}}{\left|V_{k+1/2}\right|+\left|V_{k-1/2}\right|}\right). \quad (8)$$

As a test case, the solution to a classical hydrodynamic problem - the problem of dam failure with an outflow into a filled or dry downstream - was considered (Stoker J.J., 1959, Kochin N.E., Kibel I.A., Rose N.V., 1963). It is assumed that a finite-difference grid that has a constant length step at the initial moment of time $X_{k+1/2}$-$X_{k-1/2}$=*const* $\forall k$, on the left boundary of the calculation domain, at X=0, an impermeable wall is given $V_{|x=0}=V_{|\hat{x}=0}=0$ and the dam site at the initial time t=0 coincides with the initial left-hand boundary of the calculation area, i.e., the solution of the problem corresponds to the analytical one until the downgoing wave reaches the right boundary of the calculation area $X=0$.

Here it should be noted that the system of equations (5) does not require a boundary condition on this (right) boundary in the case of dam failure with a spill into a dry channel or at shallow downstream, as the flow in its vicinity will be turbulent ($Fr_{/X=L}=\left(\frac{V^2}{gh}\right)_{/X=L}>1$). However, the layout view for the right boundary cell is not obvious and will be discussed below.

Next, consider a more general problem in which it is assumed that there is a device on the right-hand boundary of the calculation area that ensures that a constant depth is maintained on it:

$$h_{/X=L}=h_R=const. \quad (9)$$

Note that the solution to the long-wave fluid flow problem under this boundary condition is contained in the solution to the "dam break" problem (Fig. 1) at the initial depth in the tailwater $h_\infty\neq 0$.

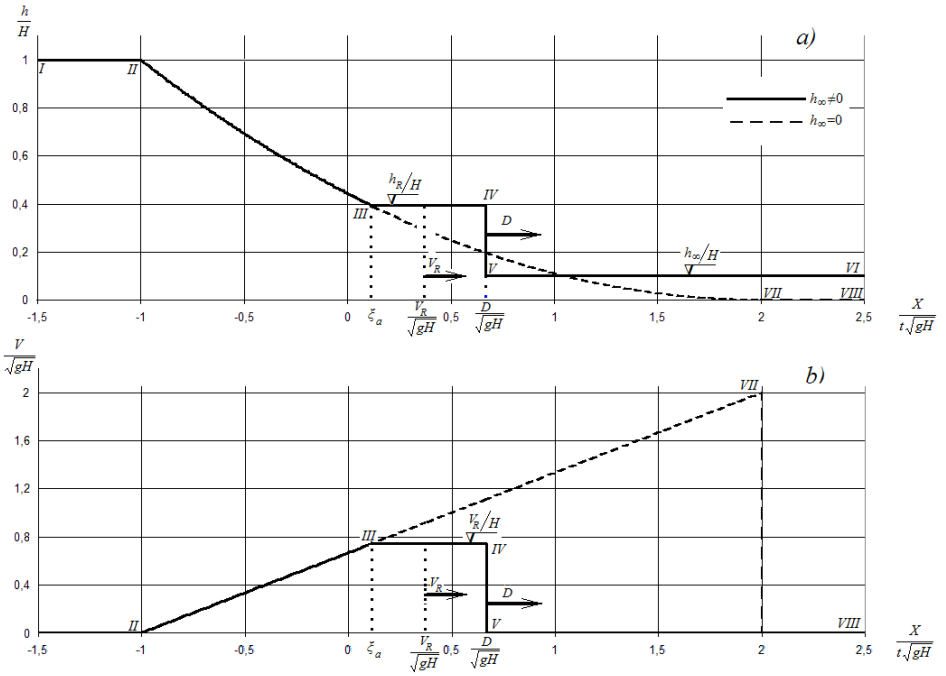

Fig. 1. Diagram of the problem solution for dam failure with a spill into the filled downstream reservoir (solid line) and onto a dry downstream (dashed line). At the initial point in time at X=0, there is a depth discontinuity in the upstream and downstream reaches - the "dam". a) - wave profile, b) - velocity graph along the flow.

I-II is undisturbed part of the upstream; *II-III* and *II-III-VII* are simple depression wave for filled and dry downstream, respectively;

III-IV is "flat" (plateau); *V-VI* is undisturbed downstream; *VII-VIII* is unflooded part of the downstream.

X is length, t is time, h is depth, V is velocity, g is acceleration of gravity, H is reservoir depth, h_∞ *is* downstream water depth, V_R and h_R are speed and water depth on the flat D – boron propagation speed.

Indeed, the line with the self-similar coordinate $V_R/\sqrt{gH}$ separates the liquid which has escaped from the reservoir and the downstream liquid which has been perturbed by the breakthrough wave, and if condition (9) is fulfilled, the analytical solution coincides with the solution of the dam failure problem, where the boundary of the calculation area moves with the velocity of water on the "flat" V_R. In this case

$$h = \begin{cases} H & \text{at} \quad X/t\sqrt{gH} < -1 \\ H\left(\frac{X/t\sqrt{gH}-2}{3}\right)^2 & \text{at} \quad -1 \le X/t\sqrt{gh} < V_R/\sqrt{gH} - \sqrt{h_R/H} \\ h_R & \text{at} \quad X/t\sqrt{gh} \ge V_R/\sqrt{gH} - \sqrt{h_R/H} \end{cases} \tag{10}$$

$$V = \begin{cases} 0 & \text{at} \quad X/t\sqrt{gH} < -1 \\ X/t\sqrt{gH} - 2 & \text{at} \quad -1 \le X/t\sqrt{gh} < V_R/\sqrt{gH} - \sqrt{h_R/H} \\ & \text{at} \quad X/t\sqrt{gh} \ge V_R/\sqrt{gH} - \sqrt{h_R/H} \end{cases} \tag{11}$$

In this case, the length of the computational domain at time *t* becomes equal to

$$L = L_{|t=0} + V_R t \tag{12}$$

Velocity at the "flat"

$$V_R = 2\left(\sqrt{gH} - \sqrt{gh_R}\right) \tag{13}$$

Froude number at the "flat"

$$Fr_R = 2\left(\sqrt{H/h_R} - 1\right). \tag{14}$$

Thus, at $h_R / H < 4/9$ the current on the shelf is turbulent, and at the position of the destroyed dam $h/H = 4/9$ and $Fr = 1$ (Stoker J.J., 1959, Kochin N.E., Kibel I.A., Rose N.V., 1963), and at $h_R / H > 4/9$ the flow at the "flat" is smooth.

In this paper, there were two variants of approximation used $h_{/X=L} = h_R = const$: at $Fr_R < 1$, from the point of view of the Saint-Venant equations, it is a boundary condition, but even with $Fr_R > 1$ it does not contradict the conditions of the task since there is such a filling of the downstream with which the depth at the "flat" is equal to h_R.

Option 1: One of the boundary conditions was that the depth in the last cell of the area at the initial moment of time is h_R, and it did not change with time, nor does the length of the last cell $\left[X_{K-1/2}, X_{K+1/2}\right]$:

$$X^1_{K+1/2} - X^1_{K-1/2} = X_{K+1/2} - X_{K-1/2},\ V^1_{K+1/2} = V^1_{K-1/2}. \tag{15}$$

Numerical experiments have shown that at $h_s / H < 4/9$ there are strong circuit pulsations in the zone of the boundary *K*-sell (Fig. 2 and 3).

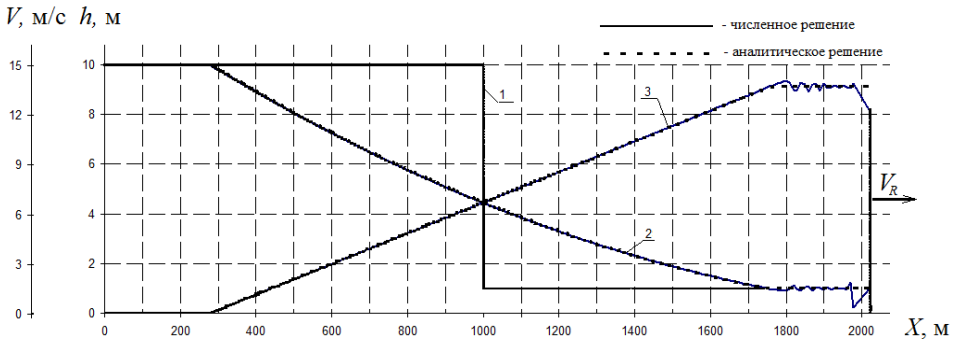

Fig. 2. Wave profile and longitudinal velocity plot when formula (2.8) is applied at the boundary point.

Legend: 1 is initial depth profile with a discontinuity at *X*=0; 2 is wave profiles: analytical and calculated according to (6); 3 is velocity graphs analytical and calculated according to (6). *H*=10 m, h_R=1 m. $Fr_R = V_R / \sqrt{gh_R} = 18 > 1$. *T*=79 sec. *K*=1000.

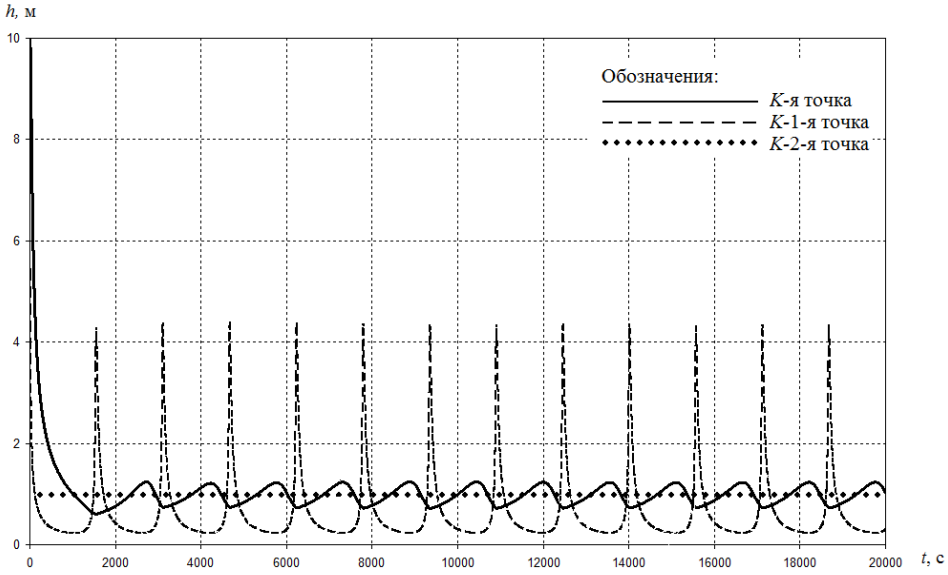

Fig. 3. The graph of the calculated depth change over time at the design points closest to the right-hand boundary. The symbols are the same as in Fig. 2.

Pulsations increase as the value of h_s / H decreases, and at small values of h_s / H , they are so strong that calculations become impossible. Note that the solution becomes unstable only in the nearest vicinity of the K-cell, which is explained by the fact that the turbulent flow "blows away" the arising oscillations and does not let them penetrate deep into the computational area.

Option 2: The velocity of the right-hand boundary of the area was calculated using the finite-difference formula:

$$V_{K+1/2}^{1} = V_{K+1/2} - \frac{\tau g}{2\Delta_{\Omega k}}\left(h_R^2 - h_K^2\right), \qquad (16)$$

which formally coincides with the third formula (2.1), that is, under the assumption that there is a "borderline" K+1-cell with specific volume $\Delta_{\Omega K+1} = \Delta_{\Omega K}$ and constant depth h_R. Numerical experiments have shown that wave flow calculations using formula (16) give satisfactory results for all values of h_R<H, including h_R =0. It can be seen that using formula (16), the results of the numerical experiment do not practically differ from the analytical solution.

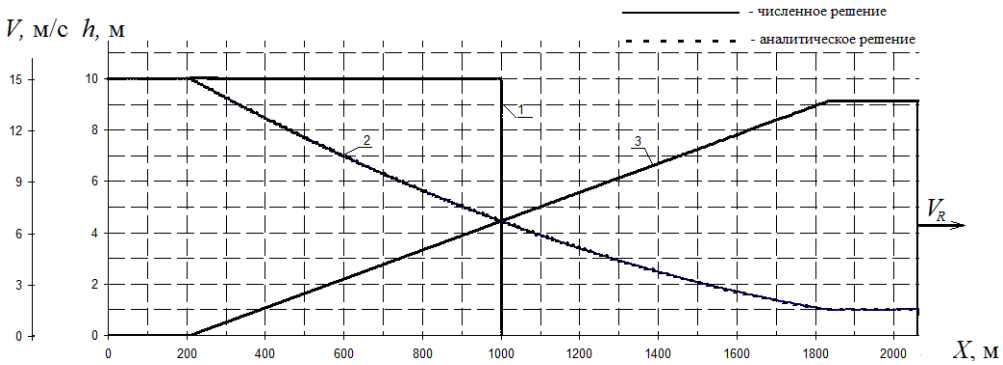

Fig. 4. Wave profile and longitudinal velocity plot when formula (15) is applied.

2. 3 Numerical implementation of the Saint-Venin equations taking into account bottom topography and friction

In the same way, as for the horizontal bottom, a spaced finite-difference grid is used (Fig. 5). To account for the bottom topography, we assume that the bottom shape is set independently of the finite-difference grid by the function $Z_b(x)$, which can be found for any x (for example, set at some node points, and for points located between them is found by interpolation).

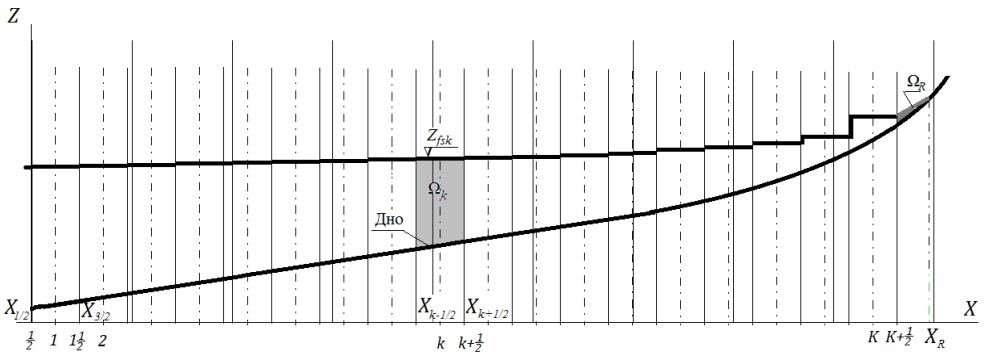

Fig. 5. Spread out finite-difference grid for non-horizontal bottom.

The following values have been determined **in the whole-numbered sections**:

- Z^1_{fsk} is water surface mark (**consider it within the interval** $\left[X^1_{k-1/2}, X^1_{k+1/2}\right]$ **constant)**
- $\Delta_{\Omega k}$ is specific (relative to flow width unit) water volume at interval $\left[X^1_{k-1/2}, X^1_{k+1/2}\right]$ ($\Delta_{\Omega k}$ does not change over time).

The following values have been determined **in the half-integer number sections**:

- $X^1_{k+1/2}$ is Eulerian coordinate of k+1/2 is line,
- $V^1_{k+1/2}$ is velocity of k+1/2-cell line.

The bottom is set independent of the moving Lagrangian finite-difference grid, e.g., on a separate time-invariant grid, so that the bottom mark of the k+1/2-cell line $Z_{bk+1/2}{}^1$ is

calculated from the Eulerian coordinate of $X^1_{k+1/2}$ the line. The finite-difference scheme (17) generalizes the above-constructed scheme (2.1) for the Saint-Venin equations in Lagrangian coordinates with a horizontal bottom to the case of an arbitrarily shaped bottom (under flat symmetry and without considering hydraulic friction):

$$\begin{cases} \int\limits_{X^1_{k-1/2}}^{X^1_{k+1/2}} \left(Z^1_{fsk} - Z_b(\xi)\right) d\xi = \int\limits_{X_{k-1/2}}^{X_{k+1/2}} \left(Z_{fsk} - Z_b(\xi)\right) d\xi = \Omega_k, \\ X^1_{k+1/2} = X_{k+1/2} + \tau V_{k+1/2}, \\ V^1_{k+1/2} = V_{k+1/2} - \dfrac{\tau g}{\Delta_{\Omega k+1} + \Delta_{\Omega k}} \left({h^1_{cmk+1}}^2 - {h^1_{cmk}}^2 \right) - \dfrac{\tau \overline{R}^1_{k+1/2}}{\Delta_{\Omega k+1} + \Delta_{\Omega k}} - \dfrac{\overline{\Theta}^1_{k+1/2}}{\Delta_{\Omega k+1} + \Delta_{\Omega k}} \end{cases} \tag{17}$$

here: h^1_{cmk} и h^1_{cmk+1} is water depths at the center of mass of the fluid compartments in the intervals $\left[X^1_{k-1/2}, X^1_{k+1/2}\right]$ and $\left[X^1_{k+1/2}, X^1_{k+3/2}\right]$ respectively (here indices "*k*" and "*k*+1" and the positions of the centers of mass of the corresponding compartments X^1_{ck} and X^1_{ck+1} (should be calculated); $\rho\,\overline{R}^1_{k+1/2}$ and $\rho\,\overline{\Theta}^1_{k+1/2}$ respectively the projections of the pressure and friction forces, referred to the unit of flow width, acting on the fluid compartment $\left[X^1_{ck}, X^1_{ck+1}\right]$. The overline over the values $\overline{R}^1_{k+1/2}$ and $\overline{\Theta}^1_{k+1/2}$ is made to distinguish between forces and their constituent distributed loads.

Consider two ways of defining $\overline{Z}^n_{fsk+1/2}$, bearing in mind that it is an arbitrary value:

Option 1. $\overline{Z}^n_{fsk+1/2} = Z^n_{fsk}$

$$V^1_{k+1/2} = V_{k+1/2} - \frac{\tau g}{\Delta_{\Omega k+1} + \Delta_{\Omega k}} \left({h^1_{ck+1}}^2 - {h^1_{ck}}^2 \right) + \tau R^1_{k+1/2} = V_{k+1/2} - \frac{\tau g}{\Delta_{\Omega k+1} + \Delta_{\Omega k}} \times$$
$$\times \left[\left(Z^n_{fsk+1} - Z^n_{bck+1}\right)^2 - \left(Z^n_{fsk} - Z^n_{bck}\right)^2 - \left(Z^n_{fsk} - Z^n_{bck+1}\right)^2 + \left(Z^n_{fsk} - Z^n_{bck}\right)^2 \right] = \tag{18}$$
$$= V_{k+1/2} - \frac{\tau g}{\Delta_{\Omega k+1} + \Delta_{\Omega k}} \left[\left(Z^n_{fsk+1} - Z^n_{bck+1}\right)^2 - \left(Z^n_{fsk} - Z^n_{bck+1}\right)^2 \right]$$

Option 2. $\overline{Z}^n_{fsk+1/2} = Z^n_{fsk+1}$

$$V^1_{k+1/2} = V_{k+1/2} - \frac{\tau g}{\Delta_{\Omega k+1} + \Delta_{\Omega k}} \left({h^1_{ck+1}}^2 - {h^1_{ck}}^2 \right) + \tau R^1_{k+1/2} = V_{k+1/2} - \frac{\tau g}{\Delta_{\Omega k+1} + \Delta_{\Omega k}} \times$$
$$\times \left[\left(Z^n_{fsk+1} - Z^n_{bck+1}\right)^2 - \left(Z^n_{fsk} - Z^n_{bck}\right)^2 - \left(Z^n_{fsk+1} - Z^n_{bck+1}\right)^2 + \left(Z^n_{fsk+1} - Z^n_{bck}\right)^2 \right] = \tag{19}$$
$$= V_{k+1/2} - \frac{\tau g}{\Delta_{\Omega k+1} + \Delta_{\Omega k}} \left[\left(Z^n_{fsk+1} - Z^n_{bck}\right)^2 - \left(Z^n_{fsk} - Z^n_{bck}\right)^2 \right]$$

Construction of a finite-difference scheme for the K-th cell, similar to (16):

The constant water level hypothesis is unsuitable for the 'overseas' liquid compartment, as plausible results are also obtained at h_R=0. This paper accepts the hypothesis that the

water level in this compartment varies linearly from Z_K^1 to Z_{fsR} in the line X_R, with the bottom mark Z_{rb} (Figure. 6).

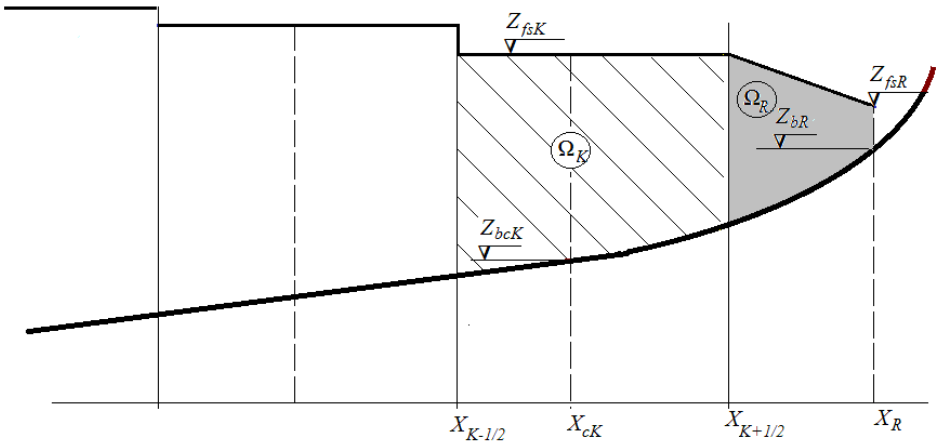

Fig. 6. Diagram of the vicinity of the boundary of the computational area with adjacent to a border compartment Ω_K and transborder compartment Ω_R. (h_R=Z_{fsR}-Z_{bR}).

The task is to determine the coordinate X_R^n, he rightmost point of the transborder liquid compartment with volume $\Delta_{\Omega R}$, given by the initial conditions. In contrast to the horizontal-bottom situation, in which coordinate X_R^1 was not involved in any way, when calculating the flow in an area with complex bottom topography, it is necessary to know X_R^1, as the pressure on the bottom side must be determined.

There are also 2 possible variants of the scheme on the boundary, which are analogous to schemes (18) and (19).

Option 1. $\overline{Z}_{fsK+1/2}^n = Z_{fsK}^n$

$$V_{K+1/2}^1 = V_{K+1/2} - \frac{\tau g}{\Delta_{\Omega K+1/1} + 2\Delta_{\Omega R}} \left[\left(Z_{fsk+1}^1 - Z_{bR}^1 \right)^2 - \left(Z_{fsk}^1 - Z_{bR}^1 \right)^2 \right] \qquad (20)$$

Option 2. $\overline{Z}_{fsK+1/2}^1 = Z_{fsK+1}^1$

$$V_{K+1/2}^1 = V_{K+1/2} - \frac{\tau g}{\Delta_{\Omega K+1/1} + 2\Delta_{\Omega R}} \left[\left(Z_{fsk+1}^1 - Z_{bck}^1 \right)^2 - \left(Z_{fsk}^1 - Z_{bck}^1 \right)^2 \right] \qquad (21)$$

In the conducted numerical experiments, the difference in results when using variants of the finite-difference scheme (18) and (19) was insignificant. However, in the case of velocity setting at K+1/2-th point, when using (20) to solve the problem of coastal slope runup, the scheme loses its stability. When using (21), the results obtained are satisfactory. Apparently, in case of coastal escarpment problem, for the boundary velocity better to use (18), because application of (19) results in instability.

3 Results and Discussion

As an example of a numerical experiment to calculate wave run-up on a slope, the problem of wave flow during an initial water level jump in an area bounded on the left by a vertical wall and on the right by a slope was considered. In this numerical experiment, friction was not considered. Figure 7 shows the wave profiles for several consecutive points in time.

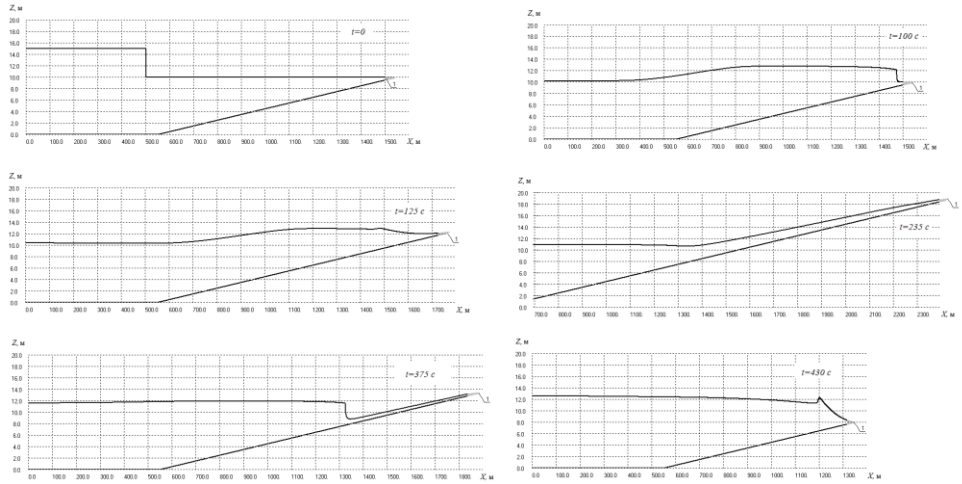

Fig. 7. Wave profiles in the area bounded on the left by the vertical wall and on the right by the shore slope at different points in time. (1 - "outboard" liquid compartment).

At the time t = 100 s, a boron is formed at the wavefront that has not collapsed even in the relatively shallow coastal area. The boron cannot move along the dry land (Belikov V.V., Norin S.V., Shkolnikov S.Ya., 2014); therefore, after the onset of coastal flooding, the boron collapses and flattens out (t = 125 c). After the maximum inundation (t=235 c), the outflow begins, with a turbulent flow regime in the upper zone of the flooded area, coupled with a calm flow at a sufficiently deep depth through the boron (t=375 c). The next period of bank inundation then begins (t=430 c).

When a rollback occurs in the vicinity of a zero-depth boundary point, the flow is formally turbulent (Fr>1), and two boundary conditions are required to solve the flow problem. One boundary condition is that h_R=0; the second condition seems to be insignificant in rollback problems since, at small values of *h,* there is no momentum entering the calculation domain (the same statement can be formulated differently: the role of the second boundary condition is played by the equality to zero of the water flow coming through the boundary q_R=0).

4 Conclusion

1. The proposed calculation method has no schematic mass diffusion, which is essential when modeling water quality.
2. Testing of the proposed finite-difference schemes showed good agreement with analytical solutions.
3. The proposed method allows modeling the transformation of the surge and tidal waves near coasts and the interaction of waves, including tsunamis, with coastal defenses, forecasting the operation of tidal HPPs, HPP-GHPPs, and the spread of pollutants.

4. Long-wave transformation studies in areas with water exchange are envisaged as a next step.

References

1. Al-Raben A. H., Gunay N. On the application of a hydrodynamic model for a limited sea area. Coastal Engineering. **17**(3–4), pp.173-194 (1992)
2. Belikov V.V., Norin S.V., Shkolnikov S.Ya. On Breaking of Polder Dams. Hydrotechnical Construction. **12**, pp. 25-34 (2014)
3. T. Buffard, T. Gallouet, J.M. Herard. Un sch´ema simple pour les ´equations de Saint-Venant, C. R. Acad. Sci. Paris S´er. I Math., **326** (3), pp.385-390 (1998)
4. J.J. Cauret, J.F. Colombeau, A.Y. LeRoux. Solutions g´en´eralis´ees discontinues de probl`emes hyperboliques non conservatifs, C. R. Acad. Sci. Paris S´er.I Math., **302**, 12, pp.435-437 (1986)
5. Chalabi Y. Qiu, Relaxation schemes for hyperbolic conservation laws with stiff source terms: application to reacting Euler equations, J. Sci. Comput., **15**(4), pp.395-416 (2000)
6. R. Courant K., Friedrichs H., Lewyt, On the Partial Difference Equations of Mathematical Physics. Mathematische Annalen **100**, pp. 32-74 (1928)
7. C.M. Dafermos. Hyperbolic conservation laws in continuum physics, Grundlehren der Mathematischen Wissenschaften (Fundamental Principles of Mathematical Sciences) **325**, Springer-Verlag, Berlin (2000)
8. C.M. Dafermos, L. Hsiao. Hyperbolic systems and balance laws with inhomogeneity and dissipation, Indiana Univ. Math. J., **31**(4), pp. 471-491 (1982)
9. D.A. Drew. Mathematical modelling of two-phase flow. Department of Mathematical Sciences, Rensselaer Polytechnic Institute, Troy, Annual Review of Fluid Mechanics, **15**, pp.261-291 (1983)
10. P. Garcia-Navarro, M.E. V´azquez-Cend´on. On numerical treatment of the source terms in the shallow water equations, Comput. and Fluids, **29**, pp. 951-979 (2000)
11. Fedotova Z.I. Substantiation of numerical method for modeling of long waves run-up on a shore. Computational Technologies. **7**(5), pp.58-76 (2002)
12. S.L.Gavrilyuk, J.Fabre. Lagrangian coordinates for a drift-flux model of a gas-liquid mixture. International Journal of Multiphase Flow. **22**(3), pp. 453-460 (1996)
13. J.F. Gerbeau, B. Perthame, Derivation of viscous Saint-Venant system for laminar shallow water; numerical validation, Discrete Contin. Dyn. Syst. Ser. **B1**(1), pp.89-102 (2001)
14. L. Gosse. Localization effects and measure source terms in numerical schemes for balance laws, Math. Comp., **71**(238), pp. 553-582 (2002)
15. N. Goutal. Finite element solution for the transcritical shallow-water equations, Math. Methods Appl. Sci., **11**(4), pp. 503-524 (1989)
16. N. Goutal, F. Maurel, Proceedings of the 2nd workshop on dam-break wave simulation, EDF-DER Report HE-43/97/016B (1997)
17. Gauckler Ph. Etudes Théoriques et Pratiques sur l'Ecoulement et le Mouvement des Eaux, vol. Tome 64, Paris, France: Comptes Rendues de l'Académie des Sciences, pp.818–822 (1867)
18. Kiselev P.G. Reference Book for Hydraulic Calculations. Fifth edition. M.-L. Energy.

p. 313 (1974)

19. Krutov A.N. Shkolnikov S.Ya. Numerical Modelling of Long Waves in the Lagrange Coordinates. S.Ya. Proc. N.N. Zubov State Oceanographic Institute. **72**, p. 250 (2022)
20. Kochin N.E., Kibel I.A., Rose N.V., Theoretical hydromechanics. Part 1. 6th edition, revised and supplemented, p.583, Moscow (1963)
21. J. A. Künge, F. M. Holly, A. Verwey. Numerical methods in river hydraulics problems. Moscow: Energoatomizdat, p. 255 (1985)
22. V.M. Lyatkher, Y.S. Yakovlev. Dynamics of Continuous Media in Calculations of Hydraulic Structures. Moscow: Energia, (1976) p. 391.
23. R.J. LeVeque, H.C. Yee. A study of numerical methods for hyperbolic conservation laws with stiff source terms, J. Comput. Phys., **86**(1), pp. 187-210 (1990)
24. S.F. Liotta, V. Romano, G. Russo. Central schemes for balance laws of relaxation type, SIAM J. Numer. Anal., **38**(4), pp. 1337-1356 (2000)
25. Manning R., 1891. On the flow of water in open channels and pipes. Transactions of the Institution of Civil Engineers of Ireland. **20**, pp. 161–207
26. McKeon B. J., Zagarola M. V., Smits A. J. A new friction factor relationship for fully developed pipe flow". Journal of Fluid Mechanics. Cambridge University Press. **538,** pp. 429–443 (2005)
27. Militeev A.N. Solution of problems of hydraulics of shallow reservoirs and pools of hydroschemes with application of numerical methods. Moscow (1982)
28. Pal Arya S., Plaie E. J. Modelling of the Stably Stratified Atmospheric Boundary Layer. Atmos. Sci. **26**(4), pp. 656-665 (1969)
29. Samarskiy A.A., Popov Yu.P., Differential methods of solving gas tasks. Textbook. - 3d edition, supplement. M.: Nauka. Gol'shov. ed. in Physics and Mathematics, (1992) p. 424.
30. Stoker J.J., Waves on water. Mathematical theory and applications. Translated from English, (1959) p. 620.
31. Wiseman J., Linear and non-linear waves. Translated from English by V.V. Zharinov. Edited by A.B. Shabanov. Edited by A.B. Shabat. p.624, Moscow (1977)
32. 3. Wolzinger N.E., Pyaskovsky R.V., Shallow Water Theory. Oceanological Problems and Numerical Methods, Gidrometeoizdat (1977) p. 206.